Colloids and Surfaces B: Biointerfaces 24 (2002) 253–264

Kinetics of ultrasonic release of doxorubicin from pluronic P105 micelles

Ghaleb A. Husseini [a], Natalya Y. Rapoport [b], Douglas A. Christensen [b], John D. Pruitt [a], William G. Pitt [a,*]

[a] *Chemical Engineering Department*, *Brigham Young Uniersity*, 350, *Clyde Building*, *Proo*, *UT* 84604, *USA* [b]

Department of Bioengineering, *Uniersity of Utah*, *Salt Lake City*, *UT* 84112, *USA* Received 14 March 2001; accepted 13 August 2001

Abstract

The aim of this research was to measure and model the kinetics of acoustic release and subsequent re-encapsulation of Doxorubicin (DOX) from Pluronic P105 micelles. A fluorescence detection ultrasound exposure chamber was used. Experimental data showed that no significant release was observed when DOX loaded in Pluronic P105 micelles was exposed to ultrasound for less than 0.1 s at a power density of 58 mW/cm^2 and a frequency of 20 kHz. Above this threshold, the amount of release was shown to increase as the pulse length increased up to 0.6 s. The same experiments showed that it requires at least 0.1 s of no ultrasound for measurable re-encapsulation to occur. Release and re-encapsulation are completed within about 0.6 s of the beginning of the ON and OFF phases of pulsed ultrasound. Several physical models and their corresponding mathematical solutions were analyzed to see which most closely fit the data. The model of zero-order release with first-order re-encapsulation appears to represent data from this polymeric system better than other models. This technique has possible applications in site-specific chemotherapy.

Keywords: Micellar drug delivery; Doxorubicin; Pulsed ultrasound; Fluorescence measurement; Kinetic models

Introduction

Chemotherapy is one of the most prevalent techniques used in the treatment of cancerous tumors. However, therapeutic agents used in chemotherapy are usually administered systemically, affecting both healthy and cancerous host cells, thus causing several unwanted side effects. Among the common chemotherapeutic agents are drugs that belong to the anthracycline family [1]. Anthracycline drugs are topoisomerase I and II inhibitors that intercalate between paired bases of the DNA, affecting many of the cell functions including DNA replication and RNA transcription [2]. Doxorubicin (DOX), a commonly used anthracycline, is not only employed in the treatment of acute leukemias and other malignant lymphomas, but is also effective against solidtumors including breast and liver carcinomas [1]. Unfortunately, like many other drugs used to treat cancer, anthracycline agents have adverse side effects including alopecia, leucopenia and bone marrow suppression [1].

One promising technique to reduce the side effects of DOX and other anthracyclines is to encapsulate these anti-neoplastic agents in polymeric micelles and trigger drug release at the tumor site. To achieve this objective, our group has been using micelles of the Pluronic family of copolymers to sequester anthracycline drugs and then trigger their release using ultrasound. Our previous work has shown that Pluronic micelles prevent encapsulated

drugs from being taken up by HL-60 cells [3–7]. Upon exposure to ultrasound, sufficient drug is released from the micelles to effectively kill these cells.

The ultrasonic enhancement of drug uptake by the cells can be attributed to one or perhaps both of the following two hypotheses, (1) ultrasound causes the release of the drug from micelles, implying that ultrasound could be focused on a localized tumor and the anti-cancer agent can be released from the micelles and delivered directly to the malignant tissues; (2) ultrasound promotes the uptake of the drug by a mechanism involving permeabilization of the cell membrane.

Several other research groups have shown that ultrasound can be used to increase the potency as well as the transport of therapeutic drugs into tumor cells, skin and biofilms [8–17]. In a previous paper [4], we reported that the self-assembled Pluronic P105 micelles can be acoustically triggered to release sequestered anthracycline drugs. The measured release increased with ultrasonic power density and decreased with ultrasonic frequency [4]. These studies were performed in the ultrasonic exposure fluorescence detection chamber described previously [4]. The apparatus is designed to measure real-time release kinetics of DOX from P105 micelles by measuring the change in fluorescence. DOX exhibits a large decrease in fluorescence when transferred from the hydrophobic core of the micelle to the surrounding aqueous solution [18]. Therefore, the release can be quantified by measuring the decrease in fluorescence intensity as ultrasound is applied at various frequencies and power densities.

:

In this paper we focus on the kinetics of acoustically activated release at 20 kHz. The kinetics of release and re-encapsulation are needed to optimize the application of ultrasound in future in vivo experiments. The 20 kHz transducer can be controlled to produce ultrasound of various duty cycles and power levels. This paper will also examine the validity of proposed kinetic models in an attempt to gain insight on the release and re-encapsulation of this drug delivery system.

2. Materials and methods

2.1. *Chemicals*

Doxorubicin was obtained from the University of Utah Hospital (SLC, UT) in a mixture with lactose as a dosage form; it was dissolved in phosphate buffered saline (PBS) and sterilized by filtration through a 0.2 m filter.

2.2. *Drug incorporation into pluronic micelles*

Pluronic P105 was obtained from BASF (Mount Olive, NJ). To prepare a stock solution, P105 was dissolved in a PBS solution to a final concentration of 10 wt%. DOX was introduced into Pluronic P105 micellar solutions by mixing stock solutions at room temperature to produce a final concentration of 6.67 g/ml. The drug has been shown to spontaneously accumulate in the hydrophobic poly(propyleneoxide) core of the Pluronic P105 [19].

2.3. *Ultrasonic exposure fluorescence detection chamber*

The chamber was built to measure the change in the level of fluorescence with and without the application of ultrasound, and to capture the real-time kinetics of drug release. Details were described previously [4]. Briefly, an argon-ion laser beam at 488 nm was directed to a cuvette containing the drug. The emissions were collected using a fiber optic collector and filtered to remove the excitation wavelength. The emissions were then quantified using a photodetector and stored in a Macintosh computer for further analysis.

2.4. *Ultrasonication*

Ultrasound at 20 kHz was generated with a sonicating probe (Sonics and Materials, Danbury, CT) inserted into the thermostatic bath near the cuvette. The 20 kHz source was programmed to deliver both continuous and pulsed ultrasound at several intensities. The ultrasonic power density inside the cuvette was estimated using a hydrophone [20]. In continuous and pulsed experiments, a power density of approximately 58 mW/cm^2 was delivered during the 'ON' time of the ultrasound exposure.

Digitized data were analyzed to calculate the percent of the drug release from micelles. The percentage release was calculated using the following equation:

$$\%\text{release} = \frac{I - I_{0\%}}{I_{100\%} - I_{0\%}} \qquad (1)$$

where $I_{100\%}$ is the fluorescence intensity recorded when the drug was in PBS, $I_{0\%}$ refers to the intensity of DOX encapsulated in Pluronic P105 without the application of ultrasound, and I is the instantaneous fluorescence level obtained during the experiment. For more details, please refer to our previous publication [4].

2.5. *Time response measurements*

A variable-speed square-wave beam chopper was used to determine the time response of the detection system. The corresponding time constants were obtained as the inverse of the slope of the log of response versus time.

2.6. *Spectra acquisition*

A CCD camera (Photometrics CH250) was used to collect DOX emissions spectra using a spectrograph (SPEX 1681 0.22 m spectrometer, entrance slit 0.5 mm) between 520 and 620 nm with and without the application of 20 kHz ultrasound at 58 mW/cm^2. The data were then analyzed for a quantifiable shift in the fluorescence spectra upon the application of ultrasound.

3. Modeling the release kinetics

The data collected show that DOX is released under ultrasonic irradiation and attains a steadystate concentration. It is re-encapsulated when ultrasound is turned off. Fig. 1 shows an idealized schematic of the release and re-encapsulation profile. The models presented in this section are an attempt to relate possible mechanisms to the observed data.

3.1. *Model* 1: *first-order release and first-order re-encapsulation*

The first model assumes that the rate of release of DOX is first order with respect to the amount of encapsulated DOX, and that the rate of re-encapsulation is first order with respect to free DOX in solution. One hypothesis of the DOX release mechanism suggests that ultrasound does not destroy micelles (so that their number is kept constant), but only perturbs the micelles and makes them 'leaky', so that they partially release their DOX. The amount released is proportional to the amount of DOX remaining in the micelles. Simultaneously, DOX is transported back into the micelles at a rate proportional to the amount of free
drug in solution (and proportional to the micelle concentration). This model assumes that the number of micelles remains constant during and after ultrasonic exposure. The mechanism is modeled as two simultaneous first-order competing events (release and re-encapsulation) using the following differential equation:

$$\left.\frac{dE}{dt}\right|_{US} = -k_{r1}E + k_{e1}F \qquad (2)$$

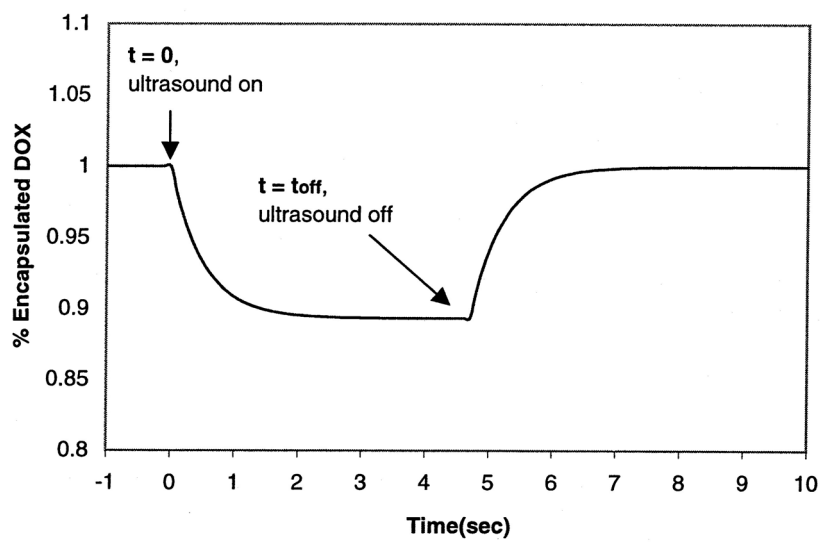

Fig. 1. An idealized schematic of the release and re-encapsulation profile.

where E is the concentration of encapsulated DOX, F is the concentration of free drug, k_{r1} and k_{e1} are the release and re-encapsulation first-order rate constants, and the subscript US indicates the application of ultrasound. The

constant k_{r1} is considered independent of time, E, and F, but it may be a function of ultrasound intensity and frequency. A simple mass balance on DOX can be used to express F in terms of E and T, the total amount of DOX in the system:

(3)

Combining equations Eqs. (2) and (3) gives:

$$\left.\frac{dE}{dt}\right|_{US} = -k_{r1}E + k_{e1}(T-E) \qquad (4)$$

Applying the initial condition that all the DOX is initially encapsulated (before ultrasonic exposure, at $t<=0$) gives the following solution:

$$\left.\frac{E(t)}{T}\right|_{US} = \left(1 - \frac{k_{e1}}{k_{e1}+k_{r1}}\right)e^{-(k_{e1}+k_{r1})t} + \frac{k_{e1}}{k_{e1}+k_{r1}} \qquad (5)$$

For this model, the release profile under ultrasound is an exponential decay function with a time constant of $1/(k_{e1}+k_{r1})$. The steady-state concentration of encapsulated drug under continuous ultrasound is $k_{e1}T/(k_{e1}+k_{r1})$. The sum of the two rate constants can be obtained from the slope of a plot of $-\ln(E(t)/T)$ versus time.

When the ultrasound is turned off (at t_{off}, see Fig. 1) release is terminated, which can be modeled by $k_{r1}=0$ in Eq. (4). Drug returns to the micelles at a rate proportional to the concentration of free drug. During this re-encapsulation period, the rate of change in the encapsulated DOX is given by:

$$\left.\frac{dE}{dt}\right|_{noUS} = k_{e1}F = k_{e1}(T-E) \qquad (6)$$

where the subscript 'noUS' indicates the absence of ultrasound. To solve this equation, the initial condition is that E (encapsulated concentration) is the value of E at the moment when the ultrasound is turned off ($E=E(t_{off})$). The solution is:

$$\left.\frac{E(t)}{T}\right|_{noUS} = \left(\frac{E(t_{off})}{T} - 1\right)e^{-k_{e1}(t-t_{off})} + 1 \qquad (7)$$

3.2. *Model* 2: *zero-order release and first-order re-encapsulation*

The second model proposes that DOX is released from micelles at a constant rate while the ultrasound is on, and the simultaneous rate of re-encapsulation is first order with respect to the concentration of free drug. The physical basis for this model is that ultrasound may create transient cavitation events that destroy micelles at a constant rate, independent of micelle concentration. DOX is released from the destroyed micelles, but can be taken up by the remaining micelles at a rate proportional to the concentration of free drug. The re-encapsulation can be either into micelles that were not destroyed, or into new micelles that form from P105 that was freed upon micelle destruction. The mathematical model is:

$$\left.\frac{dE}{dt}\right|_{US} = -k_{r2} + k_{e2}F \tag{8}$$

where k_{r2} is the rate of micelle destruction and k_{e2} is the first-order re-encapsulation rate constant.

The solution to this equation is:

$$E(t)\big|_{US} = \frac{k_{r2}}{k_{e2}} e^{-k_{e2}t} - \frac{k_{r2}}{k_{e2}} + T \tag{9}$$

Since the re-encapsulation model is first-order, when the ultrasound is turned off the re-encapsulation model and solution are identical to Eqs. (6) and (7) with k_{e2} replacing k_{e1}:

$$\left.\frac{E(t)}{T}\right|_{noUS} = \left(\frac{E(t_{off})}{T} - 1\right) e^{-k_{e2}(t - t_{off})} + 1 \tag{10}$$

3.3. *Model* 3: *first-order release and second-order re-encapsulation*

We also hypothesized a mechanism in which re-encapsulation takes place as a second-order reaction, being first-order with respect to both the number of micelles and the amount of free agent present in the system. Since the release model is first-order, the differential equation describing release is the same as in case 1, i.e. the first term on the right-hand side of Eq. (2). Re-encapsulation is modeled as the result of a free DOX molecule colliding with a micelle, resulting in the encapsulation of that molecule:

$$\text{FreeDOX+Micelle} \xrightarrow{\text{e3}} \text{EncapsulatedDOX}$$

The difference between this model and those that are first order in re-encapsulation is that the micelle concentration, $M(t)$ is not constant, but is a function of time. This model is based on the assumption that micelles are destroyed and reform both when ultrasound is applied or turned off. The rate equation describing re-encapsulation, with or without ultrasound, can be written as:

$$\frac{\mathrm{d}E}{\mathrm{d}t} = k_{\mathrm{e3}} F(t) M(t) \tag{11}$$

In order to obtain $M(t)$ in Eq. (11), we first assume that the rate of re-encapsulation is proportional to the amount of free DOX and to the number of micelles present in the system at any time. The amount of encapsulated DOX is assumed proportional to the concentration of micelles ($E(t)=M(t)$). This implies that the concentration of DOX in micelles is constant. It follows that $T=M_0$, where M_0 is the total concentration of micelles initially formed. The concentration of micelles is re-written below in terms of the formation and destruction of micelles. The micelle balance is a competition between micelle destruction (first term) and micelle formation (second term):

$$\frac{\mathrm{d}M}{\mathrm{d}t} = -k_{\mathrm{mr3}} M + k_{\mathrm{me3}} \frac{P}{N_{\mathrm{agg}}} \tag{12}$$

where P is the excess (above the CMC) free Pluronic concentration (not in micellar form) and N_{agg} is the number of Pluronic molecules per micelle, or the aggregation number. The rate of destruction of micelles upon the application of ultrasound is modeled to be first order with respect to the micelles present in the system $M(t)$. A mass balance reveals that $P/N_{\mathrm{agg}}=M_0-M(t)$, therefore, the rate of destruction and reformation of micelles can be written as follows:

$$\left.\frac{\mathrm{d}M}{\mathrm{d}t}\right|_{\mathrm{US}} = -k_{\mathrm{mr3}} M(t) + k_{\mathrm{me3}} (M_0 - M(t)) \tag{13}$$

The solution to Eq. (13) is:

$$M(t) = M_0 \left(1 - \frac{k_{\mathrm{me3}}}{k_{\mathrm{me3}} + k_{\mathrm{mr3}}}\right) e^{-(k_{\mathrm{me3}} + k_{\mathrm{mr3}})t} + \frac{k_{\mathrm{me3}} M_0}{k_{\mathrm{me3}} + k_{\mathrm{mr3}}} \tag{14}$$

Eq. (14) gives the micelle distribution as a function of time during ultrasonication. The combined release and re-encapsulation equation can be written as:

$$\left.\frac{dE}{dt}\right|_{US} = -k_{r3}E(t) + k_{e3}F(t)M(t) \qquad (15)$$

An analytical solution to this equation was attempted using an integrating factor and other techniques. However, this solution includes the term $e^{e_t}dt$, which does not have a tidy analytical solution, but can be represented by an infinite series expansion. The first three terms of the Taylor series expansion were used to evaluate the integral and a solution to Eq. (15) was obtained. The solution was too complicated to confidently regress values of k_{r3}, k_{e3}, k_{mr3}, and k_{me3}. Therefore, we made four assumptions or simplifications in order to determine the four constants. First, the rate constants for DOX release k_{r3} and for the destruction of micelles k_{mr3} are assumed to be the same, since release takes place simultaneously with micelle destruction. Second, k_{r3} can be found by measuring the initial slope of the release curve at t=0, because at this point F=0, and Eq. (15) can be solved for k_{r3}. Two remaining relationships are used, the steady state value of $E(t)$, and the initial slope of the re-encapsulation curve. At steady-state dE/dt_{noUS}=0, and therefore, the release term of Eq. (15) is equal to the re-encapsulation term:

$$k_{r3}E(\infty) = k_{e3}F(\infty)M(\infty) \qquad (16)$$

where $M(\infty)$ can be obtained from Eq. (14), and $F(\infty)$ is obtained from release experiments. The last relationship used is the initial slope of the re-encapsulation curve. When ultrasound is turned off, Eq. (15) reduces to:

$$\left.\frac{dE}{dt}\right|_{noUS} = +k_{e3}F(\infty)M(\infty) \qquad (17)$$

Using these four relationships, the four rate constants for the DOX release, re-encapsulation, micelle destruction and reformation can be regressed.

3.4. *Model* 4: *zero-order release and second-order re-encapsulation*

Model 4 assumes that release is zero-order (similar to model 2) and re-encapsulation is second-order (similar to model 3). The solution for the release and re-encapsulation are done in the same manner as model 3, with k_{r4}, k_{e4},

k_{mr4}, and k_{me4}, replacing k_{r3}, k_{e3}, k_{mr3}, and k_{me3}. The four relations that are used to evaluate these constants are the same used in model 3 with the exception of Eq. (16), which becomes:

$$k_{r4} = k_{e4} F(\infty) M(\infty) \tag{18}$$

4. Results and discussion

In order to find out which component of the detection chamber was limiting the speed of data collection, we measured the frequency response of our detection system in the presence and absence of DOX. At the high gain setting (where the data were collected), the filter failed to completely block all excitation intensity. There was sufficient 'feed-through' of the excitation beam to calculate the frequency response of the detection system. The very small amount of 'feed-through' passing through the filter was sufficiently small that it did not affect the percent release calculated using Eq. (1). The time constant was obtained as the inverse of the slope when log of detector voltage was plotted versus time. When no DOX was present, the time constant was calculated to be 7.70.1 ms. In the presence of DOX, the total time constant increased to 8.00.15 ms. The total time constant of the system can be modeled as a geometric average for τ_{DOX} and τ_{sys}:

$$\tau_{total} = \sqrt{\tau_{DOX}^2 + \tau_{sys}^2} \tag{19}$$

Using Eq. (19), τ_{DOX} = 1.94 ms. Therefore, the time constant of the detector is longer than that of DOX fluorescence. However, neither the detector nor DOX are limiting the data acquisition in our fluorescence chamber since their time constants are much shorter than 0.1 s (which is the shortest pulse length attained when using our 20 kHz transducer), and much shorter than the time constants of both data collection rates at 10 and 20 Hz.

A recent study by Kwon's group has shown DOX to associate as dimers [21]. In order to ensure that the observed decrease in fluorescence reported in our study was due to the release of DOX from the hydrophobic interior of micelles to the surrounding aqueous solution and not due to the ultrasound breaking the dimeric structure of DOX, a CCD camera and a spectrograph were used to collect spectra between 520 and 620 nm with and without the application of ultrasound. Fig. 2 shows that there is no measurable shift in the fluorescence spectrum upon the application of ultrasound. In the presence and absence of ultrasound, the ratio of the two peaks in the two spectra (labeled 1 and 2 on Fig. 2), were statistically compared using a Student's *t*-test. There was no significant difference in peak ratios when DOX was in PBS (P=0.071), nor when DOX was in 10% P105 (P=0.119).

Figs. 3 and 4 show typical pulsed data at 20 kHz and 58 mW/cm^2 obtained using the chamber described above. The decrease in the level of fluorescence corresponds to the ON phase of pulsed ultrasound and the release of the drug from micelles. The recovery of the fluorescence corresponds to the OFF phase of ultrasound (the interval between pulses), which indicates that the drug is re-encapsulated in the micelle core when ultrasound is absent. The system appears to be reversible since there is no loss of DOX emission after repeated exposures. In Fig. 3, the interval between pulses was fixed at 2 s while the pulse length was varied from 0.1 to1.6 s. In Fig. 4, the ON time was set at 2 s and the OFF time ranged between 0.1 and 1.6 s. The data presented in Fig. 3 show that if the ON time interval approaches 0.1 s, very little change in fluorescence was observed, suggesting that it takes at least 0.1 s for the ultrasound to create measurable release. The data also show that as the length of the pulse increases, the amount of release increases.

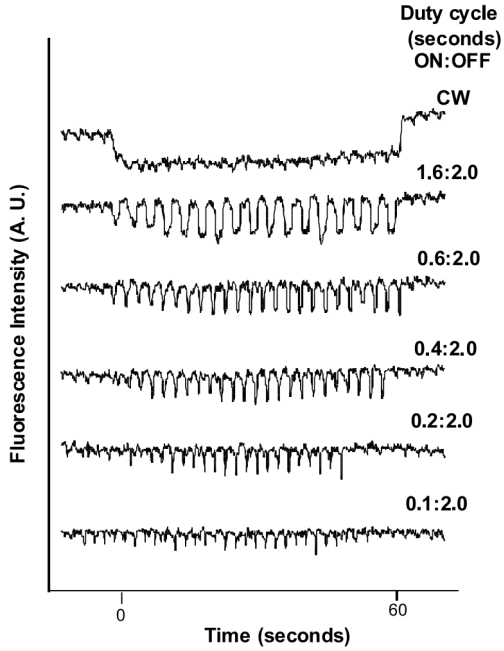

Fig. 3. Pulsed data obtained using the real time fluorescence chamber described in [4]. The time between the ultrasound pulses was kept constant at 2 s while the time of the pulse was varied between 0.1 and 1.6 s. The figure shows that there is very little change in fluorescence observed at 0.1 s and that 0.6 s is long enough for maximum release to occur.

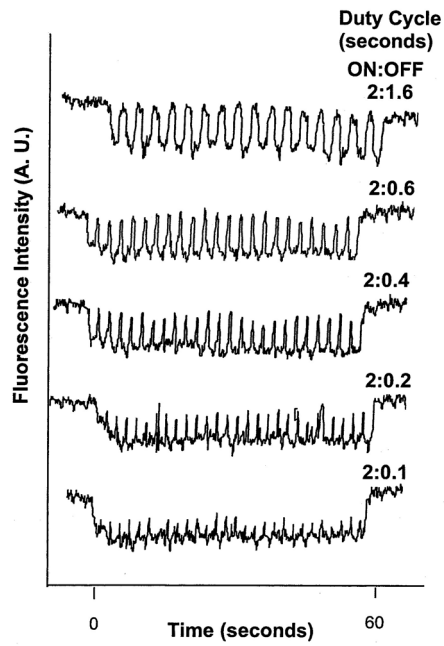

Fig. 4. Pulsed data obtained using the real time fluorescence chamber described in [4]. The 'time on' was set to 2 s and the interval between pulses was varied between 0.1 and 1.6 s. The figure shows that there is very little change in fluorescence observed if the length of the 'ultrasound off' period is 0.1 s. Complete re-encapsulation occurs in about 0.6 s.

Since the release of the drug is completed in approximately 0.6 s, pulsed instead of continuous ultrasound can be utilized in clinical applications. The advantage of using pulsed ultrasound is that less skin damage is likely to occur. In experiments with rabbits receiving ultrasonic treatment at 28.48 kHz at 300 mW/cm^2, continuous ultrasound for 24 h caused skin damage, whereas pulsed ultrasound did not [22]. Our data also suggest that the chemotherapeutic agent will be released in the target area. Upon leaving the ultrasonicated region the drug may be re-sequestered inside the micelle, thus minimizing side effects to the surrounding healthy tissues and cells.

The pulsed data also suggest that release happens slower than would be expected for simple diffusion of DOX from the core of the micelle under ultrasound. We estimated an upper limit of the diffusion coefficient using the following equation [23]:

$$r^2=6D\tau \quad (20)$$

where r is the radius of a whole micelle (including its core and shell), which can be estimated as 20 nm (as an upper limit) [24], τ is a characteristic release time estimated at about 0.1 s, and D is the

Fig. 4 shows that there is no measurable recovery in fluorescence at 0.1 s OFF, suggesting that if the interval between ultrasound pulses approaches 0.1 s, very little DOX is re-encapsulated. This observation suggests that measurable re-encapsulation requires the absence of ultrasound for at least 0.1 s. The average level of fluorescence increases as the OFF time (or the interval between pulses) increases, suggesting that the amount of re-encapsulation increases with the length of time between pulses. Release is completed within 0.6 s of the ON phase of pulsed ultrasound since the fluorescence intensity reached is the same as that reached under continuous ultrasound while re-encapsulation is completed within 0.6 s of the OFF phase of pulsed ultrasound since the recovery of the fluorescence intensity is the same as the initial intensity (at $t<=0$).

These experimental observations are vital since they provide insights into the best way this micellar drug delivery system can be administered. diffusion coefficient of DOX. Based on these values, the upper limit for the diffusion coefficient would be approximately 3.33×10^{-12} cm^2/s. Experimental values for the diffusion coefficient of DOX in solution are about 10^{-7} cm^2/s. It is doubtful that PPO would slow DOX diffusion by five orders of magnitude. Therefore, these calculations indicate that the observed release occurs much slower than could be attributed to diffusion alone. The decrease in fluorescence observed in our experiments is not a result of simple diffusion of DOX from the core of micelles beginning at t=0, but rather due to other physical phenomena. We have shown in a previous publication that the threshold of release corresponds with the observation of free radicals caused by transient cavitation [4]. This suggests that release is related to cavitation events taking place under the influence of ultrasound. We hypothesize that transient cavitation is forming temporary pores in the micelles or is destroying their structure completely, thus releasing the DOX. However, the pore formation or destruction of micelles does not appear to occur instantly when ultrasound is turned on. Thus kinetic models are more appropriate to represent the dynamics of this system, rather than a diffusion model.

In order to study the kinetics of release and re-encapsulation, ultrasound was applied continuously for 60 s in seven replicate experiments at 20 kHz and 58 mW/cm^2. An example of the change in fluorescence during release and re-encapsulation is shown in Fig. 5A and B, respectively. The shapes of these profiles suggest that they can be represented by decaying exponential functions during release and re-encapsulation. The exponential decay times of these experiments (determined as the inverse of the slope of ln(E) versus time)

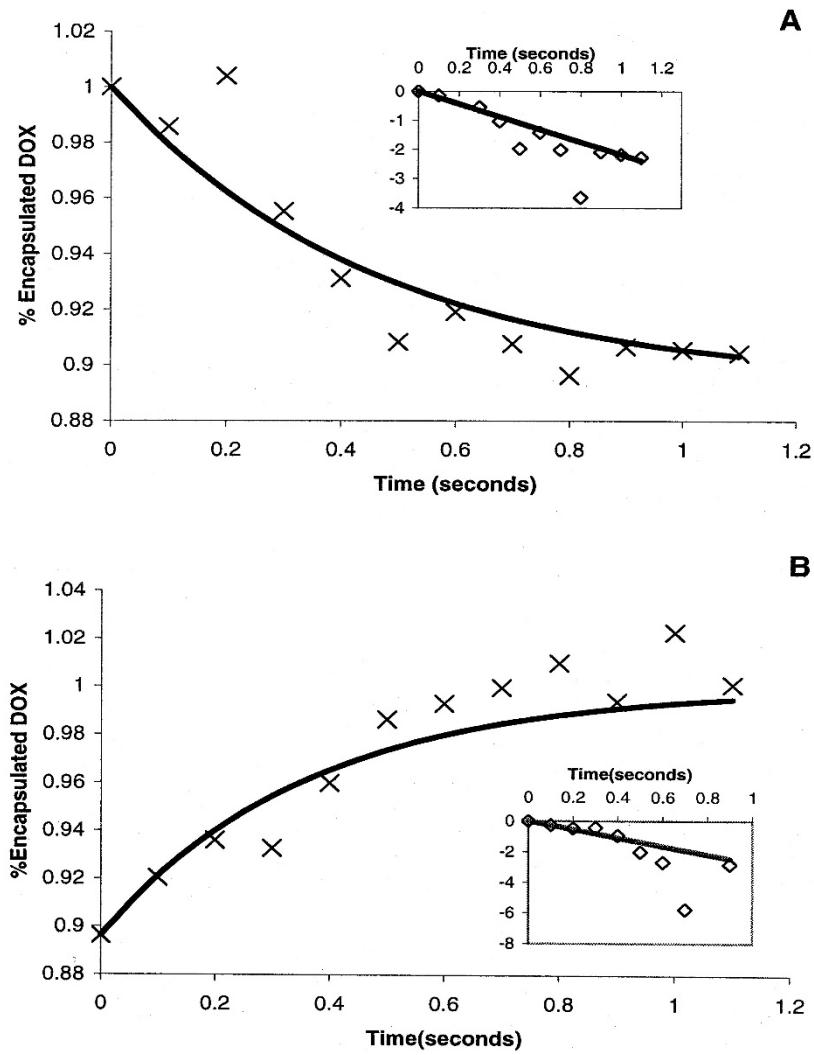

Fig. 5. Typical release and re-encapsulation data from one experiment. The solid line is the model fit using the parameters of model 2 in Table 1. The inserts are logarithmic transformations of Eqs. (7) and (9) for both the data and the proposed model fit.

Table 1
A summary of the kinetic constants obtained using the four models

Kinetic constant		Averagestandard error (S.E.) of the mean
Model 1	First order in release (k_{r1})	+0.0110.493 s^{-1}
	First order in re-encapsulation (k_{e1})	+1.9530.494 s^{-1}
Model 2	Zero order in release (k_{r2})	+0.2080.025 intensity U/s
	First order in re-encapsulation (k_{e2})	+1.9540.494 s^{-1}
Model 3	First order in release (k_{r3})	– –
	Second order in re-encapsulation (k_{e3})	
Model 4	Zero order in release (k_{r4})	– –
	Second order in re-encapsulation (k_{e4})	

–, no solution obtained.

k_{r1} is zero. But when k_{r1} is zero, a first order model is not defined. This leads us to reject the first order model and its physical analog, the leaky micelle mechanism, and to focus on models based on the destruction of micelles as a physical representation of our system.

The next three models are based on the destruction of micelles. Model 2 assumes that the micelles are destroyed at a constant rate, and DOX is re-encapsulated with first order-kinetics. The regression of data for Model 2 shows that k_{e2} is very similar to k_{e1}, which indicates that re-encapsulation is similar in both models. The observed data show that the exponential decay function of the release and re-encapsulation is similar. In this respect, Model 2 is consistent with observed data, because it predicts the exponential decay constant of both release and re-encapsulation is the same (Eq. (9) for release and Eq. (10) for re-encapsulation). Zero-order kinetics would suggest that the micelle concentration decreases until a value of zero is reached. However, release data obtained

experimentally (Figs. 3 and 4) clearly reach a plateau under sonication, suggesting that destroyed micelles are reforming and probably reach a steady state concentration.
are 0.5090.1 s during ultrasound, and 0.512 0.1 s when ultrasound was stopped. The tabulated time constants are not significantly different than each other (P0.25). The values of the kinetic constants in Eqs. (2)–(17) were regressed to fit the experimental data, and are given in Table 1. These values are the means and standard errors of the mean for regression of the models to the seven release and re-encapsulation experiments.

The data in the table indicate that the first model of first-order release and first-order re-encapsulation is probably not a realistic representation of experimental data since the value of k_{r1} is not statistically different than zero (P=0.49). Recall that the experimentally observed time constant with and without ultrasound are 0.509 and 0.512 s. This suggests that the decay time constant for the release portion of the first order model ($1/k_{e1}+k_{r1}$) is very comparable to the decay time constant for the re-encapsulation portion of the first order model ($1/k_{r1}$). Therefore, the first order model can only match the experimental data when The third model examined is first-order in release as the micelles are destroyed and first order in re-encapsulation as the micelles reform. This model is different than the leaky micelle model because it assumes that DOX is re-encapsulated in micelles whose concentration changes with time. We used the initial slopes of the release and the re-encapsulation and the steady state fluorescence level to calculate the four rate constants for DOX release (k_{r3}), re-encapsulation (k_{e3}), micelle destruction (k_{mr}) and reformation (k_{me}). No solution that could satisfy the four relationships outlined in model 3 was found, indicating that the first-order release and second-order re-encapsulation is not a valid mechanism for this micellar drug delivery system. By rejecting second order re-encapsulation, we also reject the postulate that DOX can only be re-encapsulated as the micelles reform. Similarly, Model 4 does not represent the kinetics of release and re-encapsulation adequately, since there was no solution that could fit the release and re-encapsulation data found experimentally.

Kinetics models such as these cannot reveal the mechanism of the acoustically enhanced release of DOX; however, they can be used to reject certain hypothesized mechanisms. There maybe several mathematical models that can represent the data and complex kinetics of this system. Zero-order release and first-order re-encapsulation appear to be the best representation that was attempted in this study.

5. Conclusions

The application of ultrasound causes the release of Doxorubicin from Pluronic P105 micelles. The rate at which the release and the re-encapsulation occur is rapid (on the order of tenths of seconds). This is especially evident in the case of pulsed ultrasound, in which there was release and re-encapsulation within about half a second for each pulse.

The rate of release is much slower than would be predicted for diffusion from micelles occurring instantaneously upon the application of ultrasound. Therefore, some other physical mechanism is involved, such as cavitation. The proposed model that presents the best fit of experimental data suggests that zero order release of DOX takes place, but destroyed micelles reform and both DOX and micelle concentration reach steady state. The re-encapsulation is adequately modeled as a first-order process.

The use of ultrasound to activate drug delivery is advantageous since the technique is noninvasive and can be focused on shallow or deep soft tissues throughout the body. It may have particular application to treatment of breast cancers or other localized tumor on internal organs.

Acknowledgements

The authors would like to acknowledge funding from the National Institute of Health (CA 76562).

References

[1] A.G. Gilman, J.G. Hardman, L.E. Lombard, P.B. Molinoff, R.W. Ruddon, Goodman and Gilman's the Pharmacological Basis of Therapeutics, Ninth ed., McGraw-Hill, New York, 1996.

[2] J. Nip, D.K. Strom, B.F. Fee, G. Zambetti, J.L. Cleveland, S.W. Hiebert, E2F-1 Cooperates with topoisomerase II inhibition and DNA damage to selectively augment p53-independent apoptosis, Mol. Cell Biol. 17 (3) (1997) 1049–1056.

[3] N. Rapoport, Stabilization and activation of pluronic micelles tumor-targeted drug delivery, Coll. Surf. B Biointerf. 16 (1999) 93–111.

[4] G.A. Husseini, G.D. Myrup, W.G. Pitt, D.A. Christensen, N.Y. Rapoport, Factors affecting acousticallytriggered release of drugs from polymeric micelles, J. Control. Release 69 (2000) 43–52.

[5] G.A. Husseini, R.I. El-Fayoumi, K.L. O'Neill, N.Y. Rapoport, W.G. Pitt, DNA damage induced by micellardelivered doxorubicin and ultrasound: comet assay study, Cancer Lett. 154 (2000) 211–216.

[6] N. Munshi, N. Rapoport, W.G. Pitt, Ultrasonic activated drug delivery from Pluronic P-105 micelles, Cancer Lett. 117 (1997) 1–7.

[7] N.Y. Rapoport, J.N. Herron, W.G. Pitt, L. Pitina, Micellar delivery of doxorubicin and its paramagnetic analog, ruboxyl, to HL-60 cells: effect of micelle structure and ultrasound on the intracellular drug uptake, J. Control. Release 58 (1999) 153–162.

[8] M.E. Johnson, S. Mitragotri, A. Patel, D. Blankschtein, R. Langer, Synergistic effects of chemical enhancers and therapeutic ultrasound on transdermal drug delivery, J. Pharma. Sci. 85 (7) (1996) 670–677.

[9] A.H. Saad, G.M. Hahn, Ultrasound enhanced drug toxicity on chinese hamster ovary cells in vitro, Cancer Res. 49 (1989) 5931–5934.

[10] P. Loverock, G. Ter Haar, M.G. Ormerod, P.R. Imrie, The effect of ultrasound on the cytoxicity of adriamycin, Br. J. Radiol. 63 (1990) 542–546.

[11] S. Mitragotri, D. Blankschtein, R. Langer, Ultrasoundmediated transdermal protein delivery, Science 269 (1995) 850–853.

[12] S. Mitragotri, D. Blankschtein, R. Langer, Transdermal drug delivery using low-frequency sonophoresis, Pharm. Res. 13 (3) (1996) 411–420.

[13] D. Bommannan, H. Okuyama, P. Stauffer, R.H. Guy, I. Sonophoresis, The use of high-frequency ultrasound to enhance transdermal drug delivery, Pharm. Res. 9 (4) (1992) 559–564.

[14] D. Bommannan, G.K. Menon, H. Okuyama, P.M. Elias, R.H. Guy, II Sonophoresis, Examination of the mechanism(s) of ultrasound-enhanced transdermal drug delivery, Pharm. Res. 9 (8) (1992) 1043–1047.

[15] A.M. Rediske, W.C. Hymas, R. Wilkinson, W.G. Pitt, Ultrasonic enhancement of antibiotic action on several species of bacteria, J. Gen. Appl. Microbiol. 44 (1998) 283–288.

[16] K. Tachibana, S. Tachibana, Transdermal delivery of insulin by ultrasonic vibration, J. Pharm. Pharmacol. 43 (1991) 270–271.

[17] N. Rapoport, A.I. Smirnov, A. Timoshin, A.M. Pratt, W.G. Pitt, Factors affecting the permeability of *P. aeruginosa* cell walls toward lipophilic compounds: effects of ultrasound and cell age, Arch. Biochem. Biophys. 344 (1) (1997) 114–124.

[18] N.Y. Rapoport, J.N. Herron, W.G. Pitt, L. Pitina, Micellar delivery of doxorubicin and its paramagnetic analog, ruboxyl to hl-60 cells: effect of micelle structure on the intracellular drug uptake, J. Control. Release 58 (2) (1999) 153–162.

[19] N. Rapoport, L. Pitina, Intracellular distribution and intracellular dynamics of a spin-labeled analog of doxorubicin by fluorescence and EPR spectroscopy, J. Pharm. Sci. 87 (3) (1998) 321–325.

[20] Z. Qian, R.D. Sagers, W.G. Pitt, The effect of ultrasonic frequency upon enhanced killing of *P. aeruginosa* biofilms, Annals Biomed. Eng. 25 (1) (1997) 69–
76.

[21] K. Kataoka, T. Matumoto, M. Yokoyama, T. Okano, Y. Sakurai, S. Fukushima, K. Okamoto, S. Glen, Doxorubicin-loaded poly(ethylene glycol)-poly(b-benzyl-L-aspartate): their pharmaceutical characterisitics and biological significance, J. Control. Release 64 (2000) 143–153.

[22] A.M. Rediske, B.L. Roeder, M.K. Brown, J.L. Nelson, R.L. Robison, D.O. Draper, et al., Ultrasonic enhancement of antibiotic action on *Escherichia coli* biofilms: an in vivo model, Antimicrob. Agents Chemother. 43 (5) (1999) 1211–1214.

[23] R.L. Rowley, Statistical Mechanics for Thermophysical Property Calculations, Prentice Hall PTR, Eaglewood Cliffs, NJ, 1994.

[24] J. Pruitt, G. Husseini, N. Rapoport, W. Pitt, Stabilization of pluronic P-105 micelles with an interpenetrating network of *N*,*N*-diethylacrylamide, Macromolecules 33 (25) (2000) 9306–9309.